Mechanics of Advanced Composite Structures

Semnan University

journal homepage: http://MACS.journals.semnan.ac.ir

Fluid-Structure Interaction of Vibrating Composite Piezoelectric Plates Using Exponential Shear Deformation Theory

K. Khorshidi[a,b,*], M. Karimi[a]

[a] *Department of Mechanical Engineering, Arak University, Arak, 38156-88349, Iran*
[b] *Institute of Nanosciences & Nanotechnolgy, Arak University, Arak, 38156-88349, Iran*

KEYWORDS

Galerkin method
Fluid-structure interaction
Piezoelectric plates
Exponential shear deformation theory

ABSTRACT

In this article fluid-structure interaction of vibrating composite piezoelectric plates is investigated. Since the plate is assumed to be moderately thick, rotary inertia effects and transverse shear deformation effects are deliberated by applying exponential shear deformation theory. Fluid velocity potential is acquired using the Laplace equation, and fluid boundary conditions and wet dynamic modal functions of the plate are expanded in terms of finite Fourier series to satisfy compatibility along with the interface between plate and fluid. The electric potential is assumed to have a cosine distribution along the thickness of the plate in order to satisfy the Maxwell equation. After deriving the governing equations applying Hamilton's principle, the natural frequencies of the fluid-structure system with simply supported boundary conditions are computed using the Galerkin method. The model is compared to the available results in the literature, and consequently the effects of different variables such as depth of fluid, the width of fluid, plate thickness, and aspect ratio on natural frequencies and mode shapes are displayed.

1. Introduction

Piezoelectric materials such as PZT, ZnO, and ZnS are the subset of smart materials which convert electrical energy into mechanical energy and vice versa. Piezoelectric structures extensively are applied as actuators and sensors in many branches of engineering thanks to their unique properties. These structures are quite advantageous in case of ocean engineering. Studying vibration characteristics of a structure coupled with fluid is generally known as the fluid-structure interaction (FSI) problem. In recent years, the vibration behavior of plates in contact with fluid has been in the spotlight due to the fact that having knowledge about vibrational characteristics of such structures is required in order to design ship structures, reservoirs, storage tanks, etc. Many studies have been performed to investigate the vibrations of a plate in contact with fluid [1-4]. Commonly there are three methods dealing with the FSI problems: experimental, analytical and numerical methods. Numerical methods include boundary element method and fluid finite element method, which can be employed for a large amount of FSI problems while the analytical technique is limited to some special cases.

Lame [5] was the first one who inspected the vibration behavior of the plate in contact with water. Soon after, many researches attempted to operate the effects of interaction between fluid and strucure applying various methods. Typically effects of fluid on the governing equation of structure are treated as additional force or added mass [6-12]. Free vibration of simply supported and clamped plates in contact with the fluid is studied by Khorshidi and Farhadi [13] using the Rayleigh-Ritz method. They contemplated hydrostatic pressure as initial imperfection in their formulation. Vibration analysis of laminated composite moderately thick plate for different classical boundary conditions in contact with bounded water is explored by Canales and Mantari [14]. They employed various theories of arbitrary order by applying Carrera unified formulation. Free vibration of skew and trapezoidal plates in contact with bounded fluid based on Mindlin theory using moving kriging shape functions with the element-free Galerkin method is inspected by Watts et al. [15]. Khorshidi et al. [16] did acoustic and modal tests

* Corresponding author. Tel.: +98-863-2625720; Fax: +98-86-34173450
E-mail address: k-khorshidi@araku.ac.ir

DOI: 10.22075/MACS.2019.16058.1162
Received 2018-11-29; Received in revised form 2019-02-13; Accepted 2019-02-16

in order to analyze the vibrational characteristics of thin plates with clamped supported boundary condition in contact with the rigid tank.

Kutlu et al. [17] mixed the boundary element method with finite element formulation to analyze vibrating circular and elliptical plates in interaction with the quiescent fluid. Add mass matrix can be expressed in terms of plate deflection based on their formulation. The experimental and analytical analysis for a floating sandwich plate was operated by Rezvani and Kiasat [18]. They applied first order shear deformation theory and ideal fluid hypothesis in order to derive governing equations.

Kirchhoff [19] presented classical plate theory (CPT) in 1850. Pursuant to Kirchhoff hypothesis straight lines normal to the midplane, remains straight and normal to the middle surface of the plate after deformation. Kirchhoff plate theory isn't appropriate for moderately thick plates since it neglects the transverse shear deformation stresses. In fact, it is applicable to the thin plates. First-order shear deformation theory (FSDT) [20] considers constant distribution for transverse shear deformation stresses along with the thickness of plate, which is contrary to the stress-free conditions at the bottom and top surfaces of the plate. Furthermroe, FSDT requires a shear correction factor to compensate error at top and bottom surface of the plate.

Torabizade and Fereidoon [21] presented an analytical and numerical method for the dynamic behavior of laminated composite plates using CLPT and FSDT. They concluded that the shear correction factor decreases the frequencies of the structure. Soltani et al. [22] investigated the vibration of moderately thick FG plates applying dynamic stiffness method based on FSDT. They acquired uncoupled governing equations using a new reference plane instead of the midplane of the plate. In order to get more satisfactory results, higher order shear deformation theories have been developed.

Reddy [23] was the first one who employed a parabolic shear stress distribution along the thickness of the plate. This parabolic distribution vanishes at the bottom and top surface of the plate. Hence, it requires no shear correction factor. After reddy, other researchers proposed various nonlinear distribution for transverse shear stresses along the thickness of the plate [24-28]. For instance, Sayyad and Ghugal [29, 30] devoted trigonometric and exponential distribution for capturing shear deformation effects. Khorshidi and Khodadadi [31] obtained the closed-form solution for transverse vibration of thick plates using trigonometric shear deformation theory with various boundary conditions. Khorshidi et al. [32] examined vibrational characteristics of FGM nanoplates according to exponential shear deformation theory using nonlocal theory.

Prior researches indicated that the majority of the literature dealing with FSI has done with FSDT or CPT while in the present paper exponential shear theory as a subset of modified shear deformation theory is employed. As far as it's been reported, no previous research has investigated the piezoelectric plate in contact with the fluid. Moreover, no prior studies have examined the analytical Galerkin method as a solution to the interaction between structure and fluid. In this paper, vibration analysis of piezoelectric plate in interaction with fluid is investigated. The fluid is considered to be incompressible, inviscid and irrotational and effects of sloshing are taken into account. Governing equations and boundary conditions are derived using Hamilton's principle and are solved with Galerkin method. In the result section, influences of different variables on wet frequencies are displayed.

2. Geometrical configuration

If we consider a rectangular piezoelectric plate with length a along x- axis (0<x< a), width b along y- axis (0<y<b) and thickness h in z- direction (0<z<h), in order to represent the motions of the fluid and structure, the origin of the Cartesian coordinate system is located in the bottom right-handed corner of the plate. The plate is a part of the vertical side of a rigid tank filled with a fluid, as protrayed in Fig. 1. depth and width of the fluid in the tank are b1 and c, respectively.

2.1. Exponential shear deformation theory

Exponential shear deformation theory as a member of the modified shear deformation theories considers both rotary inertia and shear deformation effects against classical plate theory.

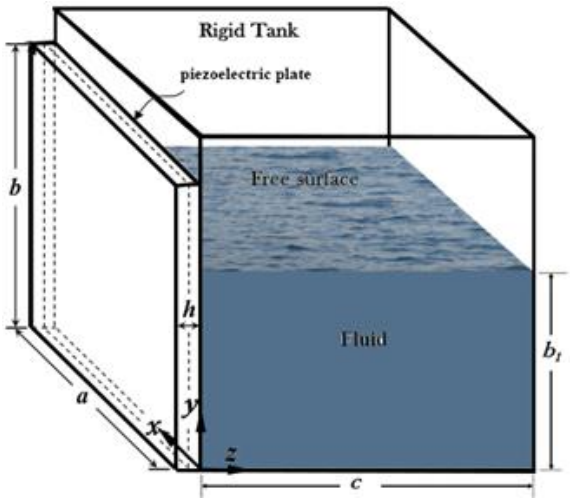

Fig. 1. fluid structure interaction of piezoelectric plate

Pursuant to this theory, displacement is in the following form [30]:

$$\begin{aligned} &u_1(x,y,z,t) = u(x,y,t) + g(z)\frac{\partial w(x,y,t)}{\partial x} + f(z)\xi(x,y,t) \\ &u_2(x,y,z,t) = v(x,y,t) + g(z)\frac{\partial w(x,y,t)}{\partial y} + f(z)\psi(x,y,t) \\ &u_2(x,y,z,t) = w(x,y,y), \mathrm{g(z)} = z + h/2, \\ &f(z) = \bar{z}\mathrm{e}^{-2\left(\frac{\bar{z}}{h}\right)^2}, \bar{z} = z + h/2 \end{aligned} \quad (1)$$

where u_1, u_2, and u_3 are displacements of an arbitrary point along x, y and z axis; u and v are in-plane displacements of the middle surface of the plate (z=-h/2); w is the out-plane displacement of the mid-plane in the plate; ξ and ψ are shear deformations measured at the mid-plane. It is clear that by vanishing f(z), classic plate theory is achieved. Based on this theory, inplane components of the displacement field include two parts; the first part which is similar to classical plate theory; the second part which is considered for counting shear deformation effects. In order to gain satisfaction from the Maxwell equation, the electric potential is approximated as follows [33]

$$\tilde{\phi}(x,y,z,t) = -Cos(\gamma\bar{z})\phi(x,y,t) \quad (2)$$

where γ=π/h and $\phi(x,y,t)$ is the electric potential in the mid-plane of the piezoelectric plate. Components of electric and strain field based on compatibility relations can be acquired as:

$$\begin{aligned} &\varepsilon_{11} = \frac{\partial u}{\partial x} - g(z)\frac{\partial^2 w}{\partial x^2} + f(z)\frac{\partial \xi}{\partial x} \\ &\varepsilon_{22} = \frac{\partial v}{\partial y} - g(z)\frac{\partial^2 w}{\partial y^2} + f(z)\frac{\partial \psi}{\partial y} \\ &\varepsilon_{12} = \frac{1}{2}\left(\left(\frac{\partial u}{\partial y} + \frac{\partial v}{\partial x}\right) - 2g(z)\frac{\partial^2 w}{\partial x \partial y} + f(z)\left(\frac{\partial \psi}{\partial x} + \frac{\partial \xi}{\partial y}\right)\right) \\ &\varepsilon_{13} = \frac{1}{2}\xi\frac{\partial f(z)}{\partial z},\ \varepsilon_{23} = \frac{1}{2}\psi\frac{\partial f(z)}{\partial z} \end{aligned} \quad (3)$$

$$\begin{aligned} &E_1 = Cos(\gamma\bar{z})\frac{\partial \phi}{\partial x}\ E_2 = Cos(\gamma\bar{z})\frac{\partial \phi}{\partial y} \\ &E_3 = -\gamma Sin(\gamma\bar{z})\phi \end{aligned} \quad (4)$$

As mentioned earlier, it can be observed from (3) that transverse shear strains have an exponential distribution simultaneously with the thickness of the plate. The constitutive relations for piezoelectric plates under the hypothesis of the plane-stress condition are shown by

$$\begin{aligned} &\sigma_{11} = \tilde{c}_{11}\varepsilon_{11} + \tilde{c}_{12}\varepsilon_{22} - \tilde{e}_{31}E_3 \\ &\sigma_{22} = \tilde{c}_{12}\varepsilon_{11} + \tilde{c}_{11}\varepsilon_{22} - \tilde{e}_{31}E_3 \\ &\sigma_{13} = 2\tilde{c}_{44}\varepsilon_{13} - \tilde{e}_{15}E_1 \\ &\sigma_{23} = 2\tilde{c}_{44}\varepsilon_{23} - \tilde{e}_{15}E_2 \\ &\sigma_{12} = 2\tilde{c}_{66}\varepsilon_{12} \end{aligned} \quad (5)$$

$$\begin{aligned} &D_1 = 2\tilde{e}_{15}\varepsilon_{13} + \tilde{\kappa}_{11}E_1 \\ &D_2 = 2\tilde{e}_{15}\varepsilon_{23} + \tilde{\kappa}_{11}E_2 \\ &D_3 = \tilde{e}_{31}\varepsilon_{11} + \tilde{e}_{31}\varepsilon_{22} + \tilde{\kappa}_{33}E_3 \end{aligned} \quad (6)$$

where $\tilde{c}_{ij}$, $\tilde{e}_{ij}$ and $\tilde{\kappa}_{ij}$ denote elastic, piezoelectric and dielectric constants associated with the plane-stress condition, respectively and are presented as

$$\begin{aligned} &\tilde{c}_{11} = c_{11} - \frac{{c_{13}}^2}{c_{33}}, \tilde{c}_{12} = c_{12} - \frac{{c_{13}}^2}{c_{33}}, \tilde{c}_{66} = c_{66} \\ &\tilde{c}_{44} = c_{44}\ \tilde{e}_{31} = e_{31} - \frac{c_{13}e_{33}}{c_{33}},\ \tilde{e}_{15} = e_{15} \\ &\tilde{\kappa}_{11} = \kappa_{11},\ \tilde{\kappa}_{33} = \kappa_{33} + \frac{{e_{33}}^2}{c_{33}} \end{aligned} \quad (7)$$

2.2. Formulation of fluid

The piezoelectric plate is partially in contact with the fluid, which is limited in a rigid tank as seen in Fig. 1. Assumptions related to the fluid can be written as:

1. The amplitude vibration of the fluid is small.
2. The hydrostatic pressure as a result of the fluid is not deliberated.
3. The fluid oscillation is contemplated to be harmonic.
4. The fluid is assumed to be ideal, i.e., incompressible, inviscid and irrotational.

In agreement with the assumptions above, the motion of the fluid is governed by the Laplace equation. Pursuant to the superposition principle, the fluid velocity potential Φ_0 contains two parts; the first part, which is related to the bulging modes, and the second one, which includes sloshing of fluid.

$$\Phi_0 = \Phi_B + \Phi_S \quad (8)$$

The fluid velocity potential applying the separation of variables method can be written as

$$\Phi_0(\mathrm{x,y,z,t}) = \phi_0(\mathrm{x,y,z})\exp(i\omega t) \quad (9)$$

where $\phi_0(\mathrm{x,y,z})$ is spatial velocity potential. According to the continuity equation, the fluid velocity potential must satisfy the Laplace equation [4]

$$\nabla^2\phi_B + \nabla^2\phi_S = 0 \rightarrow \nabla^2\phi_B = 0, \nabla^2\phi_S = 0 \quad (10)$$

The boundary conditions related to the fluid are presented by

$$
\begin{aligned}
&at\ x = 0 \Rightarrow \frac{\partial \phi_B}{\partial x} = \frac{\partial \phi_S}{\partial x} = 0\\
&at\ x = a \Rightarrow \frac{\partial \phi_B}{\partial x} = \frac{\partial \phi_S}{\partial x} = 0\\
&at\ y = 0 \Rightarrow \frac{\partial \phi_B}{\partial y} = \frac{\partial \phi_S}{\partial y} = 0\\
&at\ y = b_1 \Rightarrow \frac{\partial \phi_B}{\partial t} = 0\\
&at\ z = 0 \Rightarrow \frac{\partial \phi_B}{\partial z} = \frac{\partial w}{\partial t}\ ,\ \frac{\partial \phi_S}{\partial z} = 0
\end{aligned}
\tag{11}
$$

Applying the above boundary conditions and Eq. (10), general solution for ϕ_B and ϕ_S can be written as [8]

$$
\begin{aligned}
&\phi_B(x,y,z,t) = \sum_{l_1=0}^{\infty}\sum_{k_1=0}^{\infty} A_{l_1,k_1}(t)\\
&\cos\left(\frac{l_1\pi x}{a}\right)\left(\frac{(2k_1+1)\pi y}{2b_1}\right)\left(e^{S_1 z} + e^{S_1(2c-z)}\right)\\
&(l_1 = k_1 = 0, 1, 2, \ \dots)
\end{aligned}
\tag{12}
$$

$$
\begin{aligned}
&\phi_S(x,y,z,t) = \sum_{i_1=0}^{N_1}\sum_{j_1=0}^{M_1} B_{i_1,j_1}(t)\\
&\cos\left(\frac{i_1\pi x}{a}\right)\cosh(S_2 y)\cos\left(\frac{j_1\pi z}{c}\right)\\
&(i_1 = j_1 = 0, 1, 2, \dots, N_1, M_1)\\
&S_1 = \pi\sqrt{(l_1/a)^2 + (2k_1 + 1/(2b_1))^2}\\
&S_2 = \pi\sqrt{(i_1/a)^2 + (j_1/c)^2}
\end{aligned}
\tag{13}
$$

where $A_{l_1,k_1}(t)$ obtains, after implementing the fifth relation in Eq. (11)

$$
A_{l_1,k_1}(t) = \frac{\dfrac{coff}{ab_1}\displaystyle\int_0^a\int_0^{b_1}\begin{pmatrix}\dfrac{\partial w(x,y,t)}{\partial t}\times\\ \cos\left(\dfrac{l_1\pi x}{a}\right)\times\\ \cos\left(\dfrac{(2k_1+1)\pi y}{2b_1}\right)\end{pmatrix}dydx}{S_1(1-e^{S_1(2c)})}
\tag{14}
$$

$$
coff = \begin{cases} 1 \ \ if\ \ l_1 = k_1 = 0\\ 2 \ \ if\ \ l_1 or\ k_1 = 0\\ 4\ if\ l_1\ and\ k_1 = 0 \end{cases}
$$

Since the fluid is assumed to be ideal, the kinetic energies related to the bulging modes (T_{fB}) and sloshing modes (T_{fS}) can be written as [8]

$$
\begin{aligned}
&T_{fB} = -\frac{1}{2}\rho_F\int_0^a\int_0^{b_1}\Phi_B(x,y,0,t)\frac{\partial w(x,y,t)}{\partial t}dydx\\
&T_{fS} = -\frac{1}{2}\rho_F\int_0^a\int_0^{b_1}\Phi_S(x,y,0,t)\frac{\partial w(x,y,t)}{\partial t}dydx
\end{aligned}
\tag{15}
$$

The linearized sloshing equation at the fluid free surface can be expressed as [34]

$$
\left.\frac{\partial \Phi_B}{\partial y}\right|_{y=b_1} + \left.\frac{\partial \Phi_S}{\partial y}\right|_{y=b_1} = \left.\frac{\omega^2}{g}\Phi_S\right|_{y=b_1}
\tag{16}
$$

where g is the gravity acceleration and is considered to be g = 9.81 m/s² in all calculations. Multiplying above equation by $\rho_f\phi_S$ and integrating over the fluid surface, one can obtain:

$$
U_{\phi B} + U_{\phi S} = \omega^2 T_{\phi S}
\tag{17}
$$

in which

$$
\begin{aligned}
&U_{\phi B} = \rho_f\int_0^a\int_0^c\left(\Phi_S\frac{\partial \Phi_B}{\partial y}\right)\Big|_{y=b_1}dzdx\\
&U_{\phi S} = \rho_f\int_0^a\int_0^c\left(\Phi_S\frac{\partial \Phi_S}{\partial y}\right)\Big|_{y=b_1}dzdx\\
&T_{\phi S} = \frac{\rho_f}{g}\int_0^a\int_0^c{\Phi_S}^2\Big|_{y=b_1}dzdx
\end{aligned}
\tag{18}
$$

3. Governing equations

Strain energy (U) and kinetic energy (T) in the piezoelectric plate can be acquired as follows

$$
\begin{aligned}
&U = \frac{1}{2}\int_0^a\int_0^b\int_{-h}^0(\sigma_{11}\varepsilon_{11} + \sigma_{22}\varepsilon_{22} + 2\sigma_{12}\varepsilon_{12} +\\
&2\sigma_{13}\varepsilon_{13} + 2\sigma_{23}\varepsilon_{23} - D_1E_1 - D_2E_2 -\\
&D_3E_3)dz\,dydx\\
&T = \frac{1}{2}\rho\int_0^a\int_0^b\int_{-h}^0\left(\left(\frac{\partial u_1}{\partial t}\right)^2 + \left(\frac{\partial u_2}{\partial t}\right)^2 +\right.\\
&\left.\left(\frac{\partial u_3}{\partial t}\right)^2\right)dzdydx
\end{aligned}
\tag{19}
$$

Now governing equations of the system are derived applying Hamilton's principle

$$
\int_0^t\left(\delta T + \delta T_{fB} + \delta T_{fS} - \delta U\right)dt = 0
\tag{20}
$$

where δ denotes the first variation. Through applying Eqs. (15) and (19) and integrating by parts, the following equations are obtained:

$$
\begin{aligned}
&A_1\frac{\partial^2 u}{\partial x^2} + A_3\frac{\partial^2 \zeta}{\partial x^2} + A_4\frac{\partial^2 v}{\partial x\partial y} + A_6\frac{\partial^2 \psi}{\partial x\partial y} +\\
&A_7\frac{\partial^2 u}{\partial y^2} + A_9\frac{\partial^2 \zeta}{\partial y^2} + A_7\frac{\partial^2 v}{\partial x\partial y} + A_9\frac{\partial^2 \psi}{\partial x\partial y} -\\
&A_2\frac{\partial^3 w}{\partial x^3} - A_5\frac{\partial^3 w}{\partial x\partial y^2} + B_1\frac{\partial \phi}{\partial x} - 2A_8\frac{\partial^3 w}{\partial y^2\partial x} =\\
&\left(I_1\frac{\partial^2 u}{\partial t^2} + I_4\frac{\partial^2 \zeta}{\partial t^2} - I_2\frac{\partial^3 w}{\partial x\partial t^2}\right)
\end{aligned}
\tag{21}
$$

$$
\begin{aligned}
&A_1\frac{\partial^2 v}{\partial y^2} + A_3\frac{\partial^2 \psi}{\partial y^2} + A_4\frac{\partial^2 u}{\partial x\partial y} + A_6\frac{\partial^2 \zeta}{\partial x\partial y} +\\
&A_7\frac{\partial^2 v}{\partial x^2} + A_9\frac{\partial^2 \psi}{\partial x^2} + A_7\frac{\partial^2 u}{\partial x\partial y} + A_9\frac{\partial^2 \zeta}{\partial x\partial y} -\\
&A_2\frac{\partial^3 w}{\partial y^3} - A_5\frac{\partial^3 w}{\partial y\partial x^2} + B_1\frac{\partial \phi}{\partial y} - 2A_8\frac{\partial^3 w}{\partial x^2\partial y} =\\
&\left(I_1\frac{\partial^2 v}{\partial t^2} + I_4\frac{\partial^2 \psi}{\partial t^2} - I_2\frac{\partial^3 w}{\partial y\partial t^2}\right)
\end{aligned}
\tag{22}
$$

$$
\begin{aligned}
&-A_{10}\frac{\partial^4 w}{\partial x^4}+A_{11}\frac{\partial^3 \zeta}{\partial x^3}-A_{12}\frac{\partial^4 w}{\partial y^2\partial x^2}+\\
&A_{13}\frac{\partial^3 \psi}{\partial x^2\partial y}+B_3\frac{\partial^2 \phi}{\partial x^2}-A_{12}\frac{\partial^4 w}{\partial y^2\partial x^2}+\\
&A_{13}\frac{\partial^2 \zeta}{\partial y^2\partial x}-A_{10}\frac{\partial^4 v}{\partial y^4}+A_{11}\frac{\partial^3 \psi}{\partial y^3}+B_3\frac{\partial^2 \phi}{\partial y^2}+\\
&2A_{15}\frac{\partial^3 \zeta}{\partial y^2\partial x}-4A_{14}\frac{\partial^4 w}{\partial y^2\partial x^2}+\\
&2A_{15}\frac{\partial^3 \psi}{\partial x^2\partial y}+A_2\frac{\partial^3 u}{\partial x^3}+A_5\frac{\partial^3 v}{\partial x^2\partial y}+A_5\frac{\partial^3 u}{\partial y^2\partial x}+\\
&A_2\frac{\partial^3 v}{\partial y^3}+2A_8\frac{\partial^3 u}{\partial y^2\partial x}+2A_8\frac{\partial^3 v}{\partial x^2\partial y}=\\
&\left(-\frac{1}{2}\rho_f\left(\Phi_B(x,\mathrm{y},0,\mathrm{t})+\Phi_S(x,\mathrm{y},0,\mathrm{t})\right)+\right.\\
&I_1\frac{\partial^2 w}{\partial t^2}+I_5\frac{\partial^3 \psi}{\partial y\partial t^2}+I_2\frac{\partial^3 v}{\partial y\partial t^2}-I_3\frac{\partial^4 w}{\partial y^2\partial t^2}+\\
&\left.I_5\frac{\partial^3 \zeta}{\partial x\partial t^2}+I_2\frac{\partial^3 u}{\partial x\partial t^2}-I_3\frac{\partial^4 w}{\partial x^2\partial t^2}\right)
\end{aligned}
\tag{23}
$$

$$
\begin{aligned}
&A_3\frac{\partial^2 u}{\partial x^2}+A_{16}\frac{\partial^2 \zeta}{\partial x^2}+A_6\frac{\partial^2 v}{\partial x\partial y}+A_{17}\frac{\partial^2 \psi}{\partial x\partial y}+\\
&A_9\frac{\partial^2 u}{\partial y^2}+A_{18}\frac{\partial^2 \zeta}{\partial y^2}+A_9\frac{\partial^2 v}{\partial x\partial y}+A_{18}\frac{\partial^2 \psi}{\partial x\partial y}-\\
&A_{11}\frac{\partial^3 w}{\partial x^3}-A_{13}\frac{\partial^3 w}{\partial x\partial y^2}+B_5\frac{\partial \phi}{\partial x}-2A_{15}\frac{\partial^3 w}{\partial y^2\partial x}-\\
&A_{19}\zeta+B_7\frac{\partial \phi}{\partial x}=\left(I_6\frac{\partial^2 \zeta}{\partial t^2}+I_4\frac{\partial^2 u}{\partial t^2}-I_5\frac{\partial^3 w}{\partial x\partial t^2}\right)
\end{aligned}
\tag{24}
$$

$$
\begin{aligned}
&A_3\frac{\partial^2 v}{\partial y^2}+A_{16}\frac{\partial^2 \psi}{\partial y^2}+A_6\frac{\partial^2 u}{\partial x\partial y}+A_{17}\frac{\partial^2 \zeta}{\partial x\partial y}+\\
&A_9\frac{\partial^2 v}{\partial x^2}+A_{18}\frac{\partial^2 \psi}{\partial x^2}+A_9\frac{\partial^2 u}{\partial x\partial y}+A_{18}\frac{\partial^2 \zeta}{\partial x\partial y}-\\
&A_{11}\frac{\partial^3 w}{\partial y^3}-A_{13}\frac{\partial^3 w}{\partial y\partial x^2}+B_5\frac{\partial \phi}{\partial y}-2A_{15}\frac{\partial^3 w}{\partial x^2\partial y}-\\
&A_{19}\psi+B_7\frac{\partial \phi}{\partial y}=\left(I_4\frac{\partial^2 v}{\partial t^2}+I_6\frac{\partial^2 \psi}{\partial t^2}-I_5\frac{\partial^3 w}{\partial y\partial t^2}\right)
\end{aligned}
\tag{25}
$$

$$
\begin{aligned}
&-B_3\left(\frac{\partial^2 w}{\partial x^2}+\frac{\partial^2 w}{\partial y^2}\right)+B_5\left(\frac{\partial \zeta}{\partial x}+\frac{\partial \psi}{\partial y}\right)+\\
&B_7\left(\frac{\partial \zeta}{\partial x}+\frac{\partial \psi}{\partial y}\right)+B_3\left(\frac{\partial^2 \phi}{\partial x^2}+\frac{\partial^2 \phi}{\partial y^2}\right)+\\
&B_1\left(\frac{\partial u}{\partial x}+\frac{\partial v}{\partial y}\right)-B_9\phi-B_{10}=0
\end{aligned}
\tag{26}
$$

where A_{ij}, B_{ij} and $I_i$are given as

$$
\begin{aligned}
&\{A_1,A_4,A_7\}=\int_{-h}^{0}\{\tilde{c}_{11},\tilde{c}_{12},\tilde{c}_{66}\}\,dz\\
&\{A_2,A_5,A_8\}=\int_{-h}^{0}\{\tilde{c}_{11},\tilde{c}_{12},\tilde{c}_{66}\}\,g(z)dz\\
&\{A_3,A_6,A_9\}=\int_{-h}^{0}\{\tilde{c}_{11},\tilde{c}_{12},\tilde{c}_{66}\}\,f(z)dz\\
&\{A_{10},A_{12},A_{14}\}=\int_{-h}^{0}\{\tilde{c}_{11},\tilde{c}_{12},\tilde{c}_{66}\}\,g(z)^2dz\\
&\{A_{11},A_{13},A_{15}\}=\int_{-h}^{0}\{\tilde{c}_{11},\tilde{c}_{12},\tilde{c}_{66}\}\,g(z)f(z)dz\\
&\{A_{16},A_{17},A_{18}\}=\int_{-h}^{0}\{\tilde{c}_{11},\tilde{c}_{12},\tilde{c}_{66}\}\,f(z)^2dz\\
&\{I_1,I_2,I_3,I_4,I_5,I_6\}=\\
&\int_{-h}^{0}\rho\{1,g(z),g(z)^2,f(z),g(z)f(z),f(z)^2\}\,dz\\
&\{B_1,B_3,B_5\}=\int_{-h}^{0}\{1g(z),f(z)\}\tilde{e}_{31}\gamma Sin(\gamma\bar{z})dz
\end{aligned}
\tag{27}
$$

$$
\begin{aligned}
&B_9=\int_{-h}^{0}\tilde{\kappa}_{33}(\gamma Sin(\gamma\bar{z}))^2dz\\
&A_{19}=\int_{-h}^{0}\tilde{c}_{44}\left(\frac{\partial f(z)}{\partial z}\right)^2dz\\
&B_7=\int_{-h}^{0}\tilde{e}_{15}\frac{\partial f(z)}{\partial z}\,Cos(\gamma\bar{z})dz
\end{aligned}
$$

4. Galerkin approach

The weighted residual expressions related to the Eqs. (21) -(26) can be acquired as follows

$$
\begin{aligned}
&\int_0^b\int_0^a eq(21)\chi_1\,dxdy=0\\
&\int_0^b\int_0^a eq(22)\chi_2\,dxdy=0\\
&\int_0^b\int_0^a eq(23)\chi_3\,dxdy=0\\
&\int_0^b\int_0^a eq(24)\chi_4\,dxdy=0\\
&\int_0^b\int_0^a eq(25)\chi_5\,dxdy=0\\
&\int_0^b\int_0^a eq(26)\chi_6\,dxdy=0
\end{aligned}
\tag{28}
$$

where χ_i denotes the trial functions and are chosen in order to satisfy at least geometric boundary conditions.

Since four edges of piezoelectric are assumed to be simply supported, the mid-plane displacements (u, v, w), electric potential (ϕ) and rotations ζ and ψ are expanded by using the following expressions:

$$
\begin{aligned}
&u(x,\mathrm{y})=\sum_{n=1}^{N}\sum_{m=1}^{M}u_{m,\mathrm{n}}\,\chi_1\\
&v(x,\mathrm{y})=\sum_{n=1}^{N}\sum_{m=1}^{M}v_{m,\mathrm{n}}\,\chi_2\\
&w(x,\mathrm{y})=\sum_{n=1}^{N}\sum_{m=1}^{M}w_{m,\mathrm{n}}\,\chi_3\\
&\psi(x,\mathrm{y})=\sum_{n=1}^{N}\sum_{m=1}^{M}\psi_{m,\mathrm{n}}\,\chi_4\\
&\zeta(x,\mathrm{y})=\sum_{n=1}^{N}\sum_{m=1}^{M}\zeta_{m,\mathrm{n}}\,\chi_5\\
&\phi(x,\mathrm{y})=\sum_{n=1}^{N}\sum_{m=1}^{M}\phi_{m,\mathrm{n}}\,\chi_6
\end{aligned}
\tag{29}
$$

where $u_{m,\mathrm{n}}$, $v_{m,\mathrm{n}}$, $w_{m,\mathrm{n}}$, $\psi_{m,\mathrm{n}}$, $\zeta_{m,\mathrm{n}}$ and $\phi_{m,\mathrm{n}}$ are unknown coefficients. χ_i for simply supported boundary condition is presented as:

$$
\begin{aligned}
&\chi_1=\chi_4=\sin\left(\frac{m\pi x}{a}\right)\cos\left(\frac{n\pi y}{b}\right)\\
&\chi_2=\chi_5=\cos\left(\frac{m\pi x}{a}\right)\sin\left(\frac{n\pi y}{b}\right)\\
&\chi_3=\chi_6=\sin\left(\frac{m\pi x}{a}\right)\sin\left(\frac{n\pi y}{b}\right)
\end{aligned}
\tag{30}
$$

It's likely possible to solve the system of linear equations (28) except that expression for $B_{i1,\,j1}$ is calculated. Hence, linearized sloshing relation, i.e. Eq. (17) is added to Eq. (28). After solving theses seven equations, i.e. Eqs. (17) and (28),

eigenvalues and eigenfunctions which are related to natural frequencies and mode shapes can be obtained.

5. Validation and Convergence Studies

In order to operate the accuracy and merit of the current model, a comparison has been made with the available results existing in the literature by Khorshid and Farhadi [13], Omidezyani et al. [35,36] and Uğurlu et al. [37].

Various frequencies parameter $\varpi = \omega a^2\sqrt{\rho h/D}$ of a simply supported isotropic plate for different values of depth ratio $\frac{b_1}{b}$ are shown in Table 1. Numerical results in this table are acquired for a square isotropic plate with a=b=10 m, h=0.015 m, E=25 GPa, ρ=2400 Kg/m^3, $\nu = 0.15$ and ρ_f=1000 Kg/m^3. The flexural rigidity of the plate is denoted by $D = Eh^3/12(1-\nu^2)$. The width of the tank is assumed to be infinite, i.e. c=100 m. Based on this table there is an excellent agreement between the current model and previously published results available in the literature.

It is noteworthy to mention that the numerical results in this table are computed by vanishing electrical potential in Eqs. (21)- (26). Besides, to compute the required terms to truncate series in the Galerkin method, a convergence study is displayed in Table 2. The numerical results reported in this table are obtained for PZT4 with a=b=1 m, h=10 cm, b_1=60 cm, and c=50 cm. It can be concluded that N=M=8 is appropriate in order to ro acuqire desired accuracy.

6. Numerical Results

In this section, numerical results for vibration analysis of piezoelectric plate subjected with simply supported boundary conditions are illustrated. For all calculation, thickness of the plate is cotemplated 10 cm, and the length of the plate is taken as 1 m. Otherwise, they are specified. Moreover, the fluid existing in the tank is assumed to be water with $\rho_f = 1000$ Kg/m^3. Different properties of PZT4 which are applied in this analysis are as follows [38]

$c_{11} = 132$ GPa, $c_{12} = 71$ GPa, $c_{13} = 73$ GPa

$c_{33} = 115\ GPa$, $c_{44} = 26\ GPa$, $c_{66} = 30.5\ GPa$

ρ=7500 Kg/m^3, e_{31}=-4.1 C/m^2, e_{15}=10.5 C/m^2

e_{33}=14.1 C/m^2, κ_{11}=5.841 C/Vm, κ_{33}=7.124 C/Vm

Table 1. Dimensionless frequencies of the isotropic plate in contact with bounded fluid

Mode number	method	b_1/b 0	0.2	0.4	0.6	0.8	1
	[36]	3.1390	3.0520	2.3350	1.6390	1.2810	1.1170
	[37]	3.1917	3.1038	2.3746	1.6664	1.3030	1.1358
(1,1)	[35]	3.1690	3.0640	2.1960	1.4960	1.1730	1.0360
	[13]	3.1415	3.0127	2.0746	1.3563	1.0172	0.8565
	present	3.1393	3.0551	2.3427	1.6428	1.2822	1.1168
	[36]	7.8370	7.1860	5.7760	4.4700	3.8780	3.225
	[37]	7.9792	7.3152	5.8788	4.5498	3.9474	3.2823
(2,1)	[35]	7.9020	7.0920	5.7080	5.1740	3.9260	3.3370
	[13]	7.8528	7.9032	5.5313	4.9530	3.7329	3.1434
	present	7.8402	7.2180	5.8051	4.4952	3.8950	3.2368
	[36]	7.8370	7.6090	5.9190	5.265	3.8990	3.6870
	[37]	7.9792	7.7463	6.0251	5.3601	3.9686	3.7523
(1,2)	[35]	7.9020	7.6220	5.3820	4.0580	3.4840	3.2610
	[13]	7.8528	7.4957	5.0916	3.7884	3.2288	3.0037
	present	7.8402	7.6243	5.9346	5.3440	3.9375	3.6993
	[36]	12.525	11.501	10.153	8.9250	6.8390	5.8470
	[37]	12.7667	11.7215	10.3465	9.0951	6.9678	5.9567
(2,2)	[35]	12.680	11.400	9.9740	8.7460	6.7770	5.9420
	[13]	12.563	11.074	9.7556	8.4732	6.5259	5.6503
	present	12.5312	11.5866	10.1932	9.082	6.9234	5.8826
	[36]	15.644	13.938	11.470	9.5940	8.7310	7.5620
	[37]	15.9884	14.2176	11.6968	9.7821	8.9012	7.7085
(3,1)	[35]	15.950	13.800	12.570	10.570	9.4100	7.8480
	[13]	15.6962	13.3586	12.1332	10.2708	9.1994	7.7808
	present	15.653	14.1553	11.5324	9.7757	8.8536	7.6498
	[36]	20.312	18.259	16.686	14.198	11.994	10.462
	[37]	20.7459	18.6468	17.0397	14.4937	12.240	10.6761
(3,2)	[35]	20.690	18.100	16.680	14.470	12.660	10.720
	[13]	20.4032	17.6359	16.1027	14.1435	12.4425	10.9678
	present	20.3277	18.5814	16/9801	14/2891	12/2234	10.6087

Table 2. Convergence study of frequency parameter $\widetilde{\omega}$ for piezoelectric plate in interaction with fluid

$N_1=M_1=5$	Mode number		
	$\widetilde{\omega}_{11}$	$\widetilde{\omega}_{12}$	$\widetilde{\omega}_{22}$
N=M=4	0.5731	1.3841	2.1607
N=M=5	0.5715	1.3815	2.1599
N=M=6	0.5715	1.3811	2.1591
N=M=8	0.5715	1.3811	2.1589

Nine different mode shapes of piezoelectric plate PZT4 in contact with air and fluid are presented in Fig. 2 and 3 in order to gain more information about FSI effects.

It can be observed that wet mode shapes are distorted as a result of the interaction between the fluid and plate and this distortion is more prominent in higher modes. Mode shapes and dimensionless frequencies in these figures are acquired with a=b=1 m, h=10 cm, b_1=0.4 m and c=0.5 m.

The effects of aspect ratio (a/b) and thickness of the plate on the dimensionless frequency $\widetilde{\omega} = \omega a\sqrt{\rho/c_{11}}$ of a piezoelectric plate coupled with fluid for different values of b_1(depth of fluid) are displayed in Table 3. It is observed that overall stiffness of structure increase as the thickness of the structure of the raises. Consequently, it causes an increase in fundamental frequency. Furthermore, it can be realized that increasing aspect ratio (a/b) at a constant plate's width(b) decreases the fundamental frequency of the system. The results of this table are calculated for b=1 m and c=0.5 m.

The variations of the dimensionless fundamental frequency of piezoelectric plate coupled with fluid versus variations of fluid's depth based on classical plate theory and exponential shear deformation theory are depicted in Fig. 4.

The numerical results in this figure have been obtained for c=2 m, h=0.1 m, and a=b=1m. It is protrayedin Fig. 4 that by raising in the depth of fluid, the fundamental frequency of the system drops which is a result of the effects of fluid's kinetic energy. In fact, the existence of fluid around the plate increases the kinetic energy of the fluid-structure system and causes a raising in the overall inertia of the system.

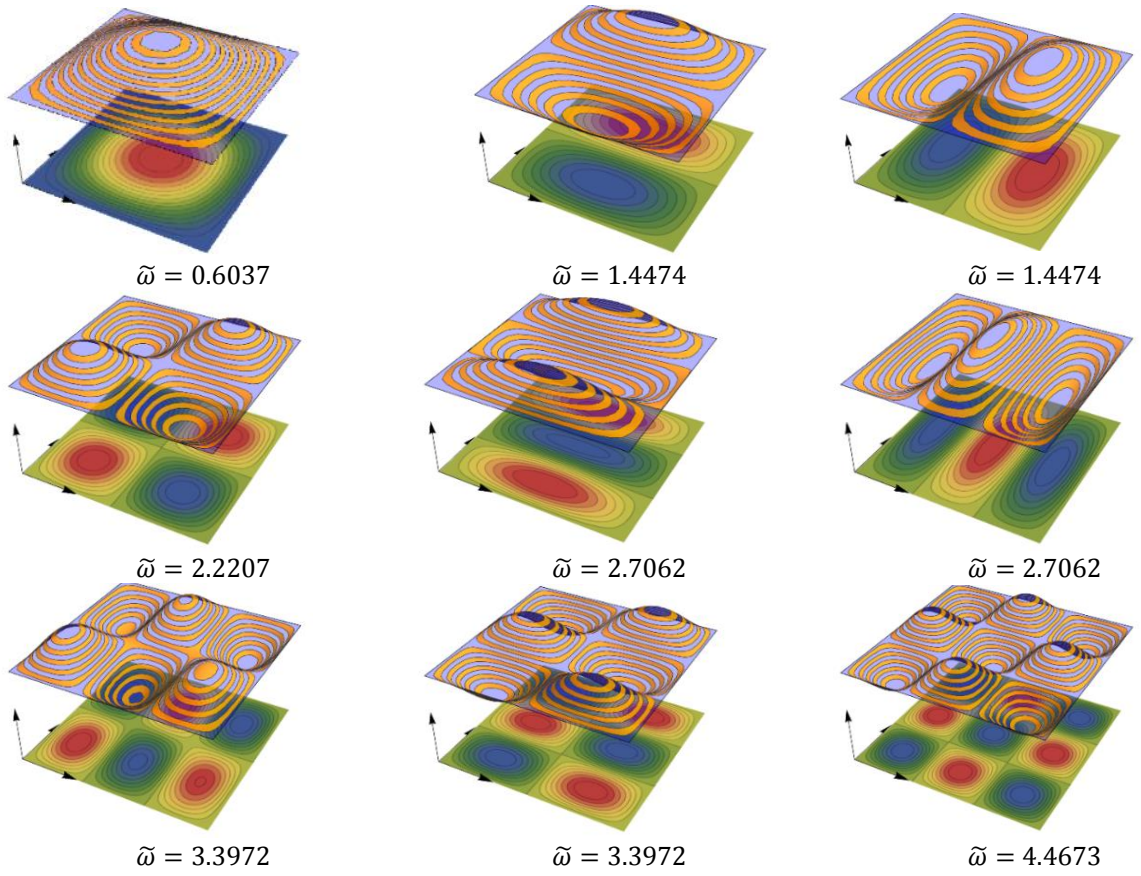

Fig. 2. mode shapes of the piezoelectric plate in contact with air

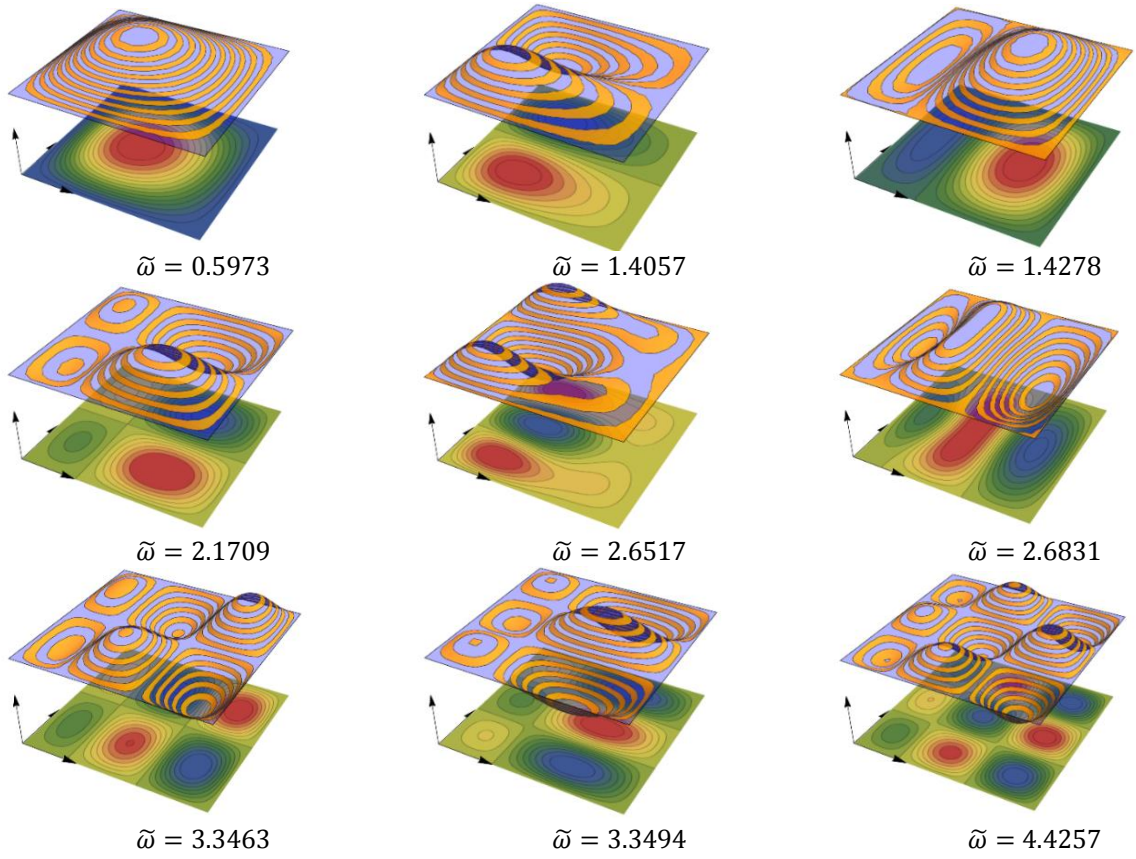

Fig. 3. mode shapes of the piezoelectric plate in contact with the fluid (b1=0.4b)

Table 3. The dimensionless fundamental frequency of piezoelectric plate in contact with the bounded fluid

$\frac{h}{b}$	$\frac{a}{b}$	b_1/b					
		0	0.2	0.4	0.6	0.8	1
0.01	0.5	0.0786	0.0776	0.0660	0.0500	0.0397	0.0333
	1	0.0629	0.0621	0.0538	0.0408	0.0318	0.0265
0.05	0.5	0.3846	0.3836	0.3720	0.3419	0.3073	0.2787
	1	0.3119	0.3111	0.3017	0.2774	0.2484	0.2248
0.1	0.5	0.7237	0.7228	0.7121	0.6819	0.6409	0.6027
	1	0.6073	0.6065	0.5973	0.5715	0.5359	0.5032
0.15	0.5	0.9997	0.9989	0.9893	0.9612	0.9207	0.8807
	1	0.8749	0.8742	0.8655	0.8401	0.8031	0.7673
0.2	0.5	1.2178	1.2171	1.2085	1.1828	1.1445	1.1055
	1	1.1103	1.1096	1.1014	1.0771	1.0407	1.0043

Fig. 5 presents the dimensionless fundamental wet frequency of a square piezoelectric plate versus width of fluid using classical plate theory and exponential shear deformation theory for $b_1 = 0.5\,m$. Pursuant to this figure, it is observed that by increasing the width of fluid, fundamental frequency raises and nears to a specific value. In other words, for high adequate values of tank's width, the assumption of infinite fluid is valid. The effect of depth of fluid on the distribution of electric potential along the y-axis at x=a/2 is depicted in Fig. 6. For a piezoelectric plate in contact with air (b1=0), the maximum value of electric potential occurs at the center of the plate, while for a piezoelectric plate in contact with the fluid, the maximum potential point deviates from the midpoint of the plate due to the fluid-structure effects.

7. Conclusions

The dynamic behavior of the piezoelectric plate (PZT4) in interaction with fluid based on exponential shear deformation theory have inspected. Exponential shear deformation theory against the classical plate theory considered rotary inertia and generated reliable results in moderately thick plates. The electric potential is assumed to have a cosine distribution in order to satisfy Maxwell equation. By inserting various energy of fluid and structure into Hamilton's principle, governing equations have derived. Governing equations by minimizing weighted

residuals in the Galerkin method based on trigonometric admissible functions have solved. High accuracy of current work has verified by comparing the present model at the special cases with previously published results. The effects of various parameters such as fluid's depth, fluid's width, thickness ratio and aspect ratio on wet natural frequencies have illustrated. Results indicate that the presence of fluid around the plate makes a distortion on the vibrational mode shapes and this distortion is more notable in higher modes. Furthermore, it is observed that increasing thickness ratio and fluid's width raise the vibrational frequencies, and increasing fluid's depth and aspect ratio reduce the vibrational frequencies. At last, it is indicated that fluid-structure coupling deviates the maximum potential point from the center of the simply supported piezoelectric plate.

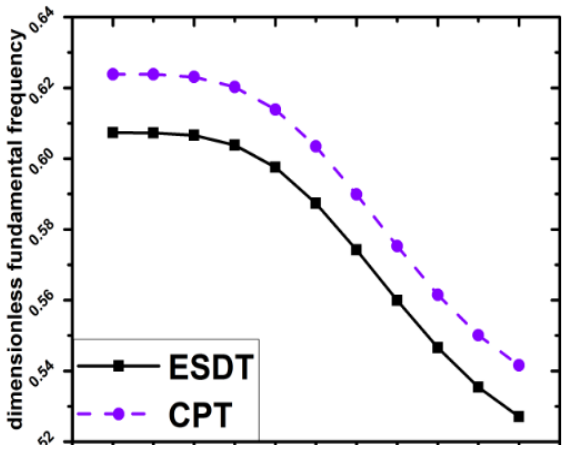

Fig. 4. variations of the dimensionless fundamental frequency of the system versus depth of fluid

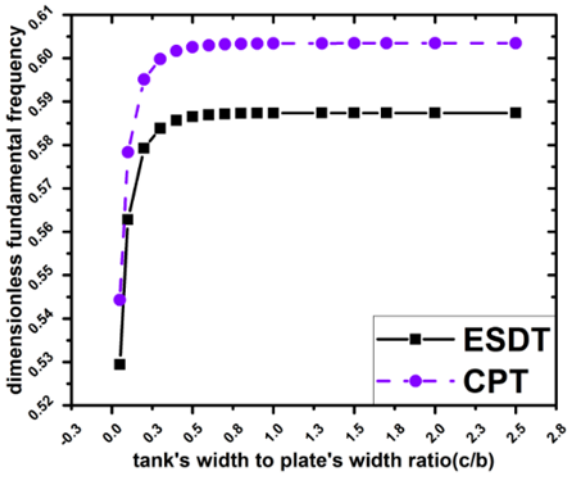

Fig. 5. variation of the dimensionless fundamental frequency of system versus tank's width

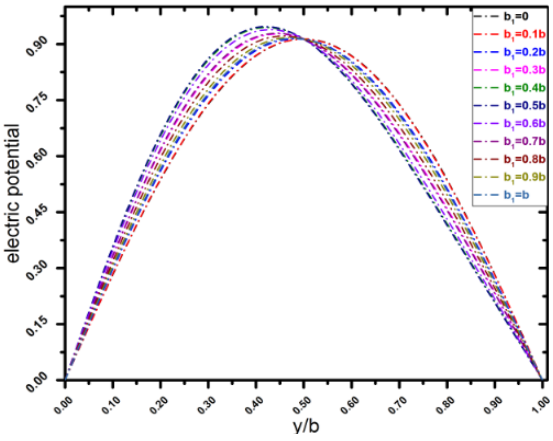

Fig. 6. variation of the electric potential distribution of system at center of piezoelectric plate (x=a/2)

References

[1] Amabili M, Kwak M. Free vibrations of circular plates coupled with liquids: revising the lamb problem. *Journal of fluids and structures* 1996; 10(7): 743-61.

[2] Watanabe E, Utsunomiya T, Tanigaki S. A transient response analysis of a very large floating structure by finite element method. *Doboku Gakkai Ronbunshu* 1998; 1998(598): 1-9.

[3] Ergin A, Uğurlu B. Linear vibration analysis of cantilever plates partially submerged in fluid. *Journal of Fluids and structures* 2003; 17(7): 927-39.

[4] Khorshidi K, Bakhsheshy A. Free natural frequency analysis of an FG composite rectangular plate coupled with fluid using Rayleigh–Ritz method. *Mechanics of Advanced Composite Structures* 2014; 1(2): 131-43.

[5] Lamb H. On the vibrations of an elastic plate in contact with water. *Proc R Soc Lond A* 1920; 98(690): 205-16.

[6] Tariverdilo S, Shahmardani M, Mirzapour J, Shabani R. Asymmetric free vibration of circular plate in contact with incompressible fluid. *Applied Mathematical Modelling* 2013; 37(1-2): 228-39.

[7] Yadykin Y, Tenetov V, Levin D. The added mass of a flexible plate oscillating in a fluid. *Journal of Fluids and Structures* 2003; 17(1): 115-23.

[8] Khorshidi K, Bakhsheshy A. Free vibration analysis of a functionally graded rectangular plate in contact with a bounded fluid. *Acta Mechanica* 2015; 226(10): 3401-23.

[9] Hashemi SH, Karimi M, Taher HRD. Vibration analysis of rectangular Mindlin plates on elastic foundations and vertically in contact with stationary fluid by the Ritz method. *Ocean Engineering* 2010; 37(2-3): 174-85.

[10] Kwak MK, Yang D-H. Free vibration analysis of cantilever plate partially submerged into a

fluid. *Journal of Fluids and Structures* 2013; 40: 25-41.
[11] Amabili M. Ritz method and substructuring in the study of vibration with strong fluid–structure interaction. *Journal of Fluids and Structures* 1997; 11(5): 507-23.
[12] Zhou D, Cheung Y. Vibration of vertical rectangular plate in contact with water on one side. *Earthquake engineering & structural dynamics* 2000; 29(5): 693-710.
[13] Khorshid K, Farhadi S. Free vibration analysis of a laminated composite rectangular plate in contact with a bounded fluid. *Composite structures* 2013; 104: 176-86.
[14] Canales FG, Mantari JL. Laminated composite plates in contact with a bounded fluid: Free vibration analysis via unified formulation. *Composite Structures* 2017; 162: 374-87.
[15] Watts G, Pradyumna S, Singha M. Free vibration analysis of non-rectangular plates in contact with bounded fluid using element free Galerkin method. *Ocean Engineering* 2018; 160: 438-48.
[16] Khorshidi K, Akbari F, Ghadirian H. Experimental and analytical modal studies of vibrating rectangular plates in contact with a bounded fluid. *Ocean Engineering* 2017; 140: 146-54.
[17] Kutlu A, Uğurlu B, Omurtag MH. A combined boundary-finite element procedure for dynamic analysis of plates with fluid and foundation interaction considering free surface effect. *Ocean Engineering* 2017; 145: 34-43.
[18] Rezvani SS, Kiasat MS. Analytical and experimental investigation on the free vibration of a floating composite sandwich plate having viscoelastic core. *Archives of Civil and Mechanical Engineering* 2018; 18(4): 1241-58.
[19] Kirchoff G. Uber das Gleichgewicht und die Bewegung einer elastischen Scheibe. *Journal fur die reine und angewandte Mathematik (Crelle's Journal)* 1850; 40: 51-88.
[20] Mindlin RD. Influence of rotatory inertia and shear on flexural motions of isotropic, elastic plates. *J appl Mech* 1951; 18: 31-8.
[21] Torabizadeh MA, Fereidoon A. A Numerical and Analytical Solution for the Free Vibration of Laminated Composites Using Different Plate Theories. *Mechanics of Advanced Composite Structures* 2017; 4(1): 75-87.
[22] Soltani M-R, Hatami S, Azhari M, Ronagh H-R. Dynamic stiffness method for free vibration of moderately thick functionally graded plates. *Mechanics of Advanced Composite Structures* 2016; 3(1): 15-30.
[23] Reddy JN. A simple higher-order theory for laminated composite plates. *Journal of applied mechanics* 1984; 51(4): 745-52.
[24] Aydogdu M. A new shear deformation theory for laminated composite plates. *Composite structures* 2009; 89(1): 94-101.
[25] Karama M, Afaq K, Mistou S. Mechanical behaviour of laminated composite beam by the new multi-layered laminated composite structures model with transverse shear stress continuity. *International Journal of solids and structures* 2003; 40(6): 1525-46.
[26] Touratier M. An efficient standard plate theory. *International journal of engineering science* 1991; 29(8): 901-16.
[27] Soldatos K. A transverse shear deformation theory for homogeneous monoclinic plates. *Acta Mechanica* 1992; 94(3-4): 195-220.
[28] Sayyad AS, Ghugal YM. Bending, buckling and free vibration responses of hyperbolic shear deformable FGM beams. *Mechanics of Advanced Composite Structures* 2018; 5(1): 13-24.
[29] Ghugal YM, Sayyad AS. Free vibration of thick orthotropic plates using trigonometric shear deformation theory. *Latin American Journal of Solids and Structures* 2011; 8(3): 229-43.
[30] Sayyad AS, Ghugal YM. Bending and free vibration analysis of thick isotropic plates by using exponential shear deformation theory. *Applied and Computational mechanics* 2012; 6(1).
[31] Khorshidi K, Khodadadi M. Precision closed-form solution for out-of-plane vibration of rectangular plates via trigonometric shear deformation theory. *Mechanics of Advanced Composite Structures* 2016; 3(1): 31-43.
[32] Khorshidi K, Asgari T, Fallah A. Free vibrations analysis of functionally graded rectangular nano-plates based on nonlocal exponential shear deformation theory. *Mechanics of Advanced Composite Structures* 2015; 2(2): 79-93.
[33] Wang Q. Axi-symmetric wave propagation in a cylinder coated with a piezoelectric layer. *International journal of Solids and Structures* 2002; 39(11): 3023-37.
[34] Amabili M. Eigenvalue problems for vibrating structures coupled with quiescent fluids with free surface. *Journal of Sound and Vibration* 2000; 231(1): 79-97.
[35] OmidDezyani S, Jafari-Talookolaei R-A, Abedi M, Afrasiab H. Vibration analysis of a microplate in contact with a fluid based on the modified couple stress theory. *Modares Mechanical Engineering* 2017; 17(2): 47-57.
[36] Omiddezyani S, Jafari-Talookolaei R-A, Abedi M, Afrasiab H. The size-dependent free vibration analysis of a rectangular Mindlin microplate coupled with fluid. *Ocean Engineering* 2018; 163: 617-29.
[37] Uğurlu B, Kutlu A, Ergin A, Omurtag M. Dynamics of a rectangular plate resting on an

elastic foundation and partially in contact with a quiescent fluid. *Journal of sound and Vibration* 2008; 317(1-2): 308-28.

[38] Ke L-L, Liu C, Wang Y-S. Free vibration of nonlocal piezoelectric nanoplates under various boundary conditions. *Physica E: Low-dimensional Systems and Nanostructures* 2015; 66: 93-106.